Research Article

For reprint orders, please contact: reprints@futuremedicine.com

Nanomedicine

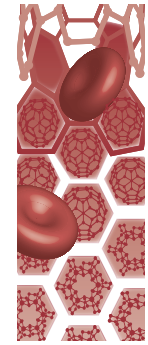

Variations of the corona HDL:albumin ratio determine distinct effects of amorphous SiO_2 nanoparticles on monocytes and macrophages in serum

Aim: We investigated monocyte and macrophage death and cytokine production induced by amorphous silica nanoparticles (SiO_2-NPs) to clarify the role of defined serum corona proteins. **Materials & methods:** The cytotoxic proinflammatory effects of SiO_2-NPs on human monocytes and macrophages were characterized in no serum, in fetal calf serum and in the presence of purified corona proteins. **Results:** In no serum and in fetal calf serum above approximately 75 µg/ml, SiO_2-NPs lysed monocytes and macrophages by plasma membrane damage (necrosis). In fetal calf serum below approximately 75 µg/ml, SiO_2-NPs triggered an endolysosomal acidification and caspase-1-dependent monocyte death (pyroptosis). The corona high-density lipoproteins:albumin ratio accounted for the features of the SiO_2-NPs in serum. **Discussion:** Corona high-density lipoproteins are a major determinant of the differential cytotoxic action of SiO_2-NPs on monocytes and macrophages.

Original submitted 15 October 2013; Revised submitted 20 January 2014

KEYWORDS: amorphous silica nanoparticle • HDL • macrophage • monocyte • nanoparticle protein corona • pyroptosis

Chiara Fedeli[1,2], Daniela Segat[3,4], Regina Tavano[1,2], Giorgia De Franceschi[1], Patrizia Polverino de Laureto[1], Elisa Lubian[5], Francesco Selvestrel[5], Fabrizio Mancin[‡5] & Emanuele Papini[‡*1,2]

[1]Interdepartmental Research Center for Innovative Biotechnologies, Università di Padova, via U Bassi 58/B, I-35131, Padova, Italy

[2]Department of Biomedical Sciences, Università di Padova, via U Bassi 58/B, I-35131, Padova, Italy

[3]Department of Biology, Università di Padova, via U Bassi 58/B, I-35131, Padova, Italy

[4]Institute for Rare Diseases 'Mauro Baschirotto', via Bartolomeo Bizio 1, 36023 Costozza di Longare (Vicenza), Italy (current address)

[5]Department of Chemistry, Università di Padova, via Marzolo 1, I-35131, Padova, Italy

*Author for correspondence:
Tel.: +39 0498276301
Fax: +39 0498276159
emanuele.papini@unipd.it

‡These authors contributed equally

In this study, we built on our previous observation that amorphous silica nanoparticles (NPs; SiO_2-NPs) kill human monocytes and macrophages at doses approximately ten-times lower than those required to affect epithelial cells or lymphocytes [1]. These cells internalize SiO_2-NPs in acidic compartments much better than nonphagocytes, thus reaching an intracellular load more easily that results in catastrophic inflammatory death, characterized by lysis and release of proinflammatory cytokines, among which are TNF-α, IL-6 and IL-1β. Cell death and inflammation are relevant adverse reactions also to other NPs, and are hallmarks of many diseases, including cancer, silicosis and chronic inflammations. Pyroptosis, a programmed death occurring in myeloid cells characterized by lysis and by the secretion of powerful proinflammatory cytokines, is mediated by the cytosolic cysteine protease caspase-1 in inflammasomes [2,3]. Activated caspase-1 determines the conversion of inactive pro-IL-1β and pro-IL-18 into mature/active IL-1β/IL-18 and the processing of other ill-known intracellular proteins [4], eventually inducing cell lysis. Among the microbial and tissue-derived factors that activate inflammasome-forming nucleotide-binding oligomerization domain (NOD)-like receptors [5,6], micro- and nano-sized particulates are of particular pathological relevance. Cell-internalized particulates destabilize the phagolysosomal membrane, determining the cytosolic leak of cathepsin B, or related proteases, which in turn activate NLRP3 [3]. Since the lysosomotropic NH_3 and the vacuolar-type H^+-ATPase (V-ATPase) inhibitor bafilomycin AI (BafAI) prevent NLRP3 activation induced by micro- or nano-particles in macrophages and dendritic cells [7–12], the acidity of particle-entrapping endosomes (pH ~4.5–5) may play a role in mediating cellular effects [6].

Future Medicine part of fsg

The above-summarized data warn on the risk that industrial-derived NPs and nanotheranostics may trigger the proinflammatory death of phagocytes [13]. Understanding the physicochemical principles involved in these phenomena may be of decisive importance for the successful development of nanomedicine.

Another critical aspect of NP bioactivities is the formation of the 'protein corona' [14–18], a layer of biomolecules adsorbed on the NP surface in the host biofluids, believed to substantially change the NPs' behaviours [19–21]. Coating of NPs with hydrophilic polymers is normally used to minimize the corona formation and to obtain 'stealth' NPs with higher stability and longer half life *in vivo* [22]. Some studies suggest that the protein corona simply masks the NP's surface [23,24]. Other evidence points to a positive modulation of NP activity by specific corona components [25,26].Therefore, direct evidence of cell-specific positive effects induced by well-defined serum components of the corona would be of paramount importance.

To jointly address the two important issues of the cytotoxic/inflammatory effects of NPs and of their modulation by the protein corona, we investigated the interaction of amorphous SiO_2-NPs (either commercial 25-nm diameter Ludox® TM-40 particles [Sigma-Aldrich, MO, USA] or 32-nm diameter Stöber NPs made in-house) with primary human monocytes and macrophages in the absence of proteins and in media containing fetal calf serum (FCS) or purified serum proteins. Although SiO_2-based nanomaterials are proposed in nanomedicine, amorphous SiO_2-NPs induce cytotoxic and proinflammatory effects *in vitro* and *in vivo* [27–29]. In addition, SiO_2-NPs have a higher tendency to bind monocytes/macrophages compared with epithelial cells in serum, triggering cytotoxic and proinflammatory effects [1]. Human exposure to nanostructured amorphous silica is also likely, due to its use as a food additive [30].

Table 1. Physicochemical characterization of the nanoparticles used.

Parameter	Ludox®	Stöber
Hydrodynamic size (diameter, nm)	25 ± 3	32 ± 4
Polydispersity index	0.12	0.19
Size (diameter, nm)	24 ± 2	30 ± 4
Zeta-potential (mV)	-16	-18
%Si-OH (^{29}Si NMR; %)	98	93

The values after the '±' symbol are the standard deviation of the Gaussian distribution of the particles sizes.
%Si-OH: Degree of condensation expressed as percentage of Si-OH (silanol) groups over the total number of Si-O units, as calculated by ^{29}Si NMR spectra; NMR: Nuclear magnetic resonance.

Our results show that macrophages and monocytes are comparably affected by SiO_2-NPs in the absence of serum, via a common mechanism involving direct plasma membrane damage and lysis, pointing to passive cell necrosis, paralleled by cytokine release. On the contrary, in serum, a cell death mechanism with the general characteristics of pyroptosis occurred in monocytes but was surprisingly not evident in macrophages. Eventually, we prove that the dispersion state and the differential cellular activity of SiO_2-NPs in serum is determined essentially by the ratio between high-density lipoprotein (HDL) and human serum albumin (HSA) in the corona.

Materials & methods

Dynamic light scattering measurements, cytokine detection, western blotting, ATP assay, real-time PCR analysis, in-gel digestion, protein identification and database search were carried out by standard procedures; for more information please see the Supplementary Material (see online at www.futuremedicine.com/doi/suppl/10.2217/NNM.14.22).

Cells

Mononuclear cells and macrophages were obtained from buffy coats of healthy donors by Ficoll-Hypaque™ (GE Healthcare, Milan, Italy) and Percoll® (GE Healthcare) centrifugation, as described in [31] (see Supplementary Material for further details).

FACS analysis

Cells seeded onto 24-well plates (2×10^6/well) were incubated at 37°C for 4–20 h with fluorescein isothiocyanate-labeled Stöber NPs (0–300 µg/ml) in normal medium plus or minus FCS. In some cases, cells were preincubated for 1 h with 12.5-nM BafAI (Sigma-Aldrich) or 200-µM *N*-acetyl-tyrosyl-valyl-alanyl-aspartyl chloromethyl ketone (Ac-YVAD-CMK; Cayman Chemical, MI, USA) before NP treatment, and further incubated with the same inhibitors (see Supplementary Material for further details).

3-(4,5-dimethylthiazol-2-yl)-5-(3-carboxymethoxyphenyl)-2-(4-sulfophenyl)-2H-tetrazolium & lactate dehydrogenase assays

Monocytes and macrophages (1.5×10^5 cells/well) seeded onto 96-well plates were tested with CellTiter 96® AQueous One Solution Reagent (Promega, Milan, Italy), or CytoTox 96® Non-Radioactive Cytotoxicity Assay (Promega; see Supplementary Material for further details).

Confocal microscopy analysis

Monocytes and macrophages (2×10^6 cells/well) seeded on cover glasses were washed with phosphate-

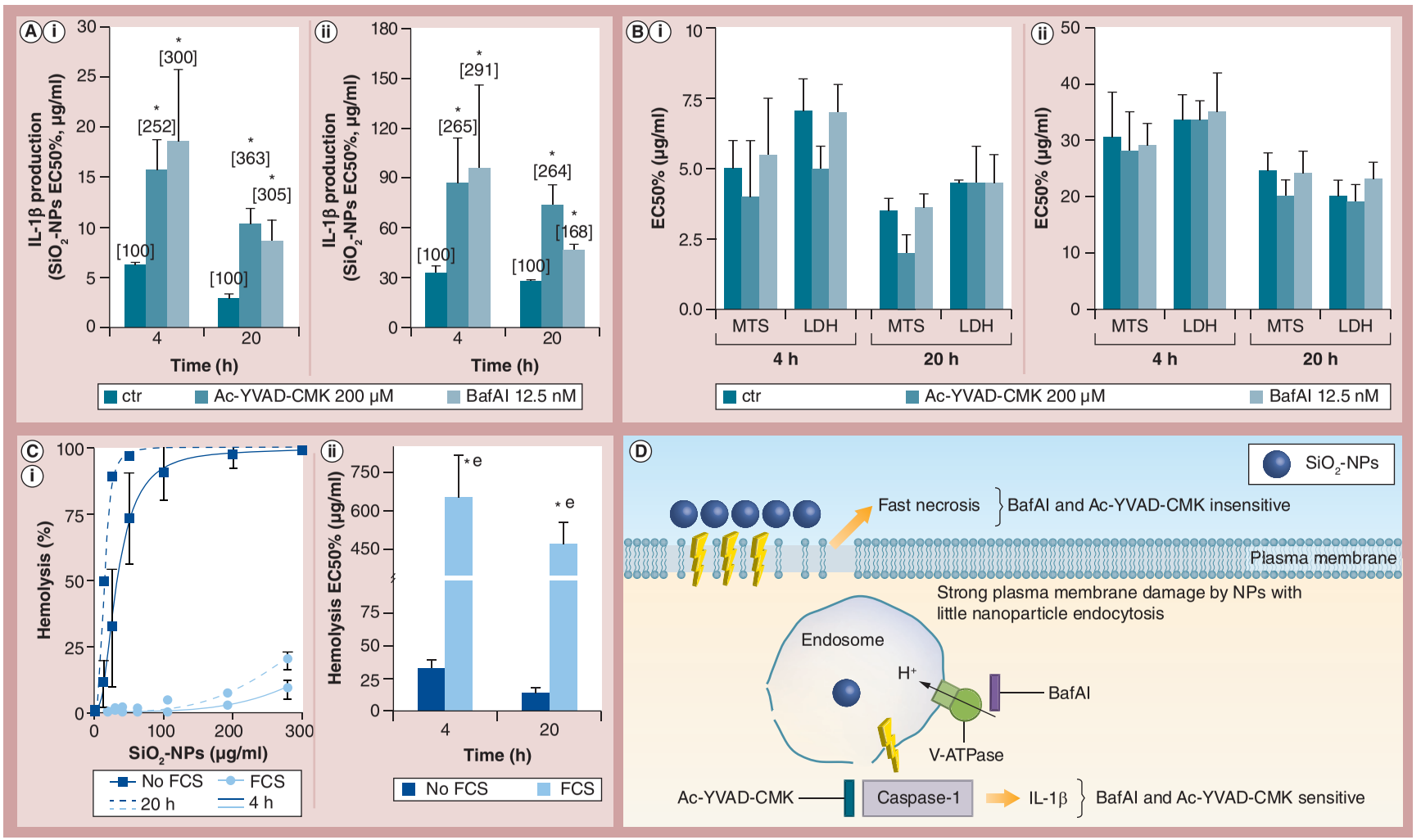

Figure 1. Cytotoxicity and IL-1β release induced by amorphous silica nanoparticles in monocytes and macrophages in the absence of serum. **(A)** Efficacies of IL-1β production by **(A,i)** monocytes and **(A,ii)** macrophages incubated in serum-free medium with Ludox® TM-40 SiO_2-NPs (Sigma-Aldrich, MO, USA) in the presence of the indicated inhibitors. Data are expressed as the effect concentration (50%; EC50%) obtained from experiments exemplified in Supplementary Figure S2A. Data are means (n = 5) ± standard error of the mean (SE). The values in square brackets show the percentage variation of EC50% compared with the value obtained in the absence of inhibitors in each condition (taken as 100%). *Indicates significant differences ($p < 0.05$ vs control in the corresponding condition). **(B)** Bars represent the SiO_2-NP EC50% values in serum-free medium resulting from the indicated cytotoxicity assays (exemplified in Supplementary Figure S3A) after incubation of **(B,i)** monocytes and **(B,ii)** macrophages at 37°C for 4 and 20 h with Ludox TM-40 SiO_2-NPs alone (ctr) or in the presence of Ac-YVAD-CMK 200 μM or BafAI 12.5 nM (1-h preincubation). Data are the means ± SE of four independent experiments run in duplicate. **(C)** Hemolytic activity of Ludox TM-40 SiO_2-NPs at 37°C for 4 and 20 h in the absence or presence of 10% FCS. Representative curves were obtained by nonlinear logistic fit of means from **(C,i)** triplicates and **(C,ii)** synthetic histograms showing EC50%. Data are the means ± SE (n = 4). 'e' indicates that values are extrapolated for >300 μg/ml). *Indicates significant differences ($p < 0.05$ FCS vs no serum). **(D)** Two independent mechanisms induced by SiO_2-NPs leading to either cytotoxicity or IL-1β production in no serum. The lightning bolt symbols indicate the damage/disruption of the lipid bilayer of membranes. Ac-YVAD-CMK: *N*-acetyl-tyrosyl-valyl-alanyl-aspartyl chloromethyl ketone; BafAI: Bafilomycin AI; EC50%: SiO_2-NP dose resulting in half-maximal effect; FCS: Fetal calf serum; SiO_2-NP: Amorphous silica nanoparticle; V-ATPase: Vacuolar-type H^+-ATPase.

fsg future science group
10.2217/NNM.14.22

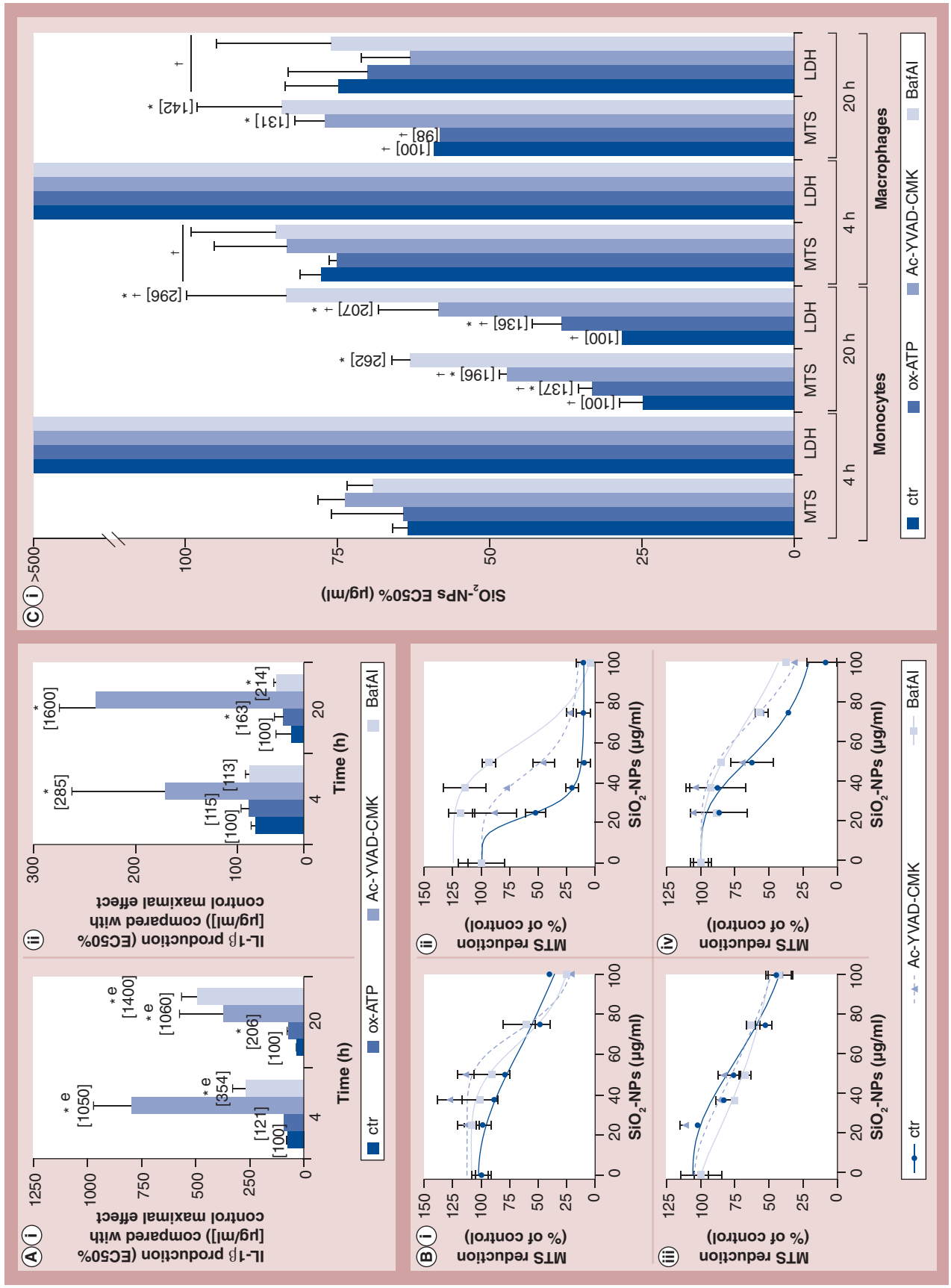
A i
IL-1β production (EC50% control maximal effect [pg/ml]) compared with
Time (h)
ctr
ox-ATP
Ac-YVAD-CMK
BafAI
A ii
IL-1β production (EC50% control maximal effect [pg/ml]) compared with
Time (h)
B i
MTS reduction (% of control)
SiO2-NPs (μg/ml)
B ii
MTS reduction (% of control)
SiO2-NPs (μg/ml)
B iii
MTS reduction (% of control)
SiO2-NPs (μg/ml)
B iv
MTS reduction (% of control)
SiO2-NPs (μg/ml)
C i
SiO2-NPs EC50% (μg/ml)
MTS
LDH
4 h
20 h
Monocytes
Macrophages
ctr
ox-ATP
Ac-YVAD-CMK
BafAI

Figure 2. Cytotoxicity and IL-1β release induced by amorphous silica nanoparticles in monocytes and macrophages in 10% fetal calf serum (cont.; see previous page). (A) The effects of the indicated inhibitors (ox-ATP 100 μM, Ac-YVAD-CMK 200 μM or BafAI 12.5 nM) on the SiO_2-NP-induced release of IL-1β from **(A,i)** monocytes and **(A,ii)** macrophages, expressed as EC50%. Data are the means ± standard error of the mean (SE; n = 5) calculated from dose–response curves (Supplementary Figure S2B). 'e' indicates that values are extrapolated. The values in square brackets show the percentage variation of EC50% compared with the value obtained in the absence of inhibitors in each condition (taken as 100%). *Indicates significant differences ($p < 0.05$ vs ctr in the corresponding condition). **(B)** MTS assay dose–response curves after incubation of **(B,i & B,ii)** monocytes and **(B,iii & B,iv)** macrophages at 37°C with Ludox® TM-40 SiO_2-NPs (Sigma-Aldrich, MO, USA) alone (ctr) or in the presence of Ac-YVAD-CMK 200 μM or BafAI 12.5 nM (1-h preincubation) for **(B,i &B,iii)** 4 h and **(B,ii & B,iv)** 20 h. Data are the means ± SE, run in triplicates. **(C)** SiO_2-NP EC50% values (MTS and LDH assays) after cellular treatment in the absence or presence of the indicated inhibitors. Data are the means ± SE (n = 4). The values in square brackets represent the percentage variation of EC50% compared with the value obtained in the absence of inhibitors in each condition (taken as 100%). *Indicates significant differences ($p < 0.05$ vs the corresponding ctr value [no inhibitors] in the same condition). †Indicates significant differences ($p < 0.05$) between EC50% values after 20 vs 4 h of incubation in the same cell type.
Ac-YVAD-CMK: *N*-acetyl-tyrosyl-valyl-alanyl-aspartyl chloromethyl ketone; BafAI: Bafilomycin AI; ctr: Control; EC50%: Effect concentration (50%); SiO_2-NP dose resulting in half-maximal effect; MTS: 3-(4,5-dimethylthiazol-2-yl)-5-(3-carboxymethoxyphenyl)-2-(4-sulfophenyl)-2H-tetrazolium; ox-ATP: Oxidized ATP; SiO_2-NP: Amorphous silica nanoparticle.

buffered saline (PBS) and incubated at 37°C for 1.5 h with different doses of fluorescein isothiocyanate-labeled Stöber NPs (25–300 μg/ml), in medium without serum or containing purified HSA 5 mg/ml (Sigma-Aldrich) or purified human HDL 35 μg/ml (Calbiochem, Darmstadt, Germany), or 10% FCS. Cells were then incubated at 37°C for 30 min with LysoTracker® Red (Invitrogen, Monza, Italy; 75 nM) in serum-free medium, rinsed with PBS and analyzed with a SP2 Leica confocal microscope (Leica, Wetzlar, Germany). Tiff file images were processed with standard imaging programs. NP/LysoTracker colocalization was estimated by Image J software and expressed as Pearson's (Rr) correlation coefficient [32], after sampling a minimum of ten fields randomly chosen from slides from separate independent experiments (n = 3).

Hemolysis assay

Human erythrocytes were obtained from human blood of healthy volunteers after elimination of buffy coats, washed in PBS plus citrate 5 mM, and further treated with PBS alone or supplemented with HSA 5 mg/ml, HDL 35 μg/ml and 10% FCS at pH 5 or 7.2. After incubation at 37°C (4–20 h) in the same buffers with different SiO_2-NP doses (5–500 μg/ml) in triplicate, samples were centrifuged (1500 rpm for 5 min) and supernatant absorbance determined at 450 nm using a Biotrak™ II reader spectrophotometer (GE Healthcare; in some cases, the hemolysis efficacy of SiO_2-NPs was expressed as effect concentration (50%; EC50%) after nonlinear logistic fitting as for other cytotoxic assays).

Data processing & statistical analysis

All mathematical and statistical analyses were performed using the analysis and statistic packages of the Microcal Origin 8 software (see Supplementary Material for further details).

Results

Characterization of SiO_2-NP cytotoxicity on monocytes & macrophages in the absence of serum

The relevant features of SiO_2-NPs, either from commercial sources (Ludox TM-40) or prepared by us and labeled with fluorescein to trace the NPs in cells by the Stöber reaction, are similar (Table 1 & Supplementary Figure S1).

As mentioned above, it is accepted that particulates activate caspase-1 by inducing the cytosolic leak of cathepsin B from acidic compartments after endocytosis. Consistently, the neutralization of endolysosomal pH by BafA1 [33,34] and the inhibition of caspase-1 by Ac-YVAD-CMK [35] determined a similar and significant reduction of IL-1β secretion induced by SiO_2-NPs in both monocytes and macrophages (EC50% increase ranging from 1.7- to 3.6-fold; Figure 1A & Supplementary Figure S2A). Control experiments indicated that these inhibitors have no significant or poor effects on cell viability and metabolism in all of the experimental conditions used in this work (see Supplementary Table S1). However, the cell death induced by SiO_2-NPs in no serum was not prevented by the inhibition of V-ATPase and caspase-1. This death phenomenon is characterized by the concomitant rapid decrease of mitochondrial metabolism (3-[4,5-dimethylthiazol-2-yl]-5-[3-carboxymethoxyphenyl]-2-[4-sulfophenyl]-2H-tetrazolium [MTS] test) and by cellular lysis (lactate dehydrogenase release test; Figure 1B), typical of passive necrosis. In agreement with this hypothesis (exemplified in Figure 1D), erythrocytes, lacking endocytosis, strongly and rapidly release hemoglobin when treated with SiO_2-NPs in no serum (Figure 1C).

10.2217/NNM.14.22

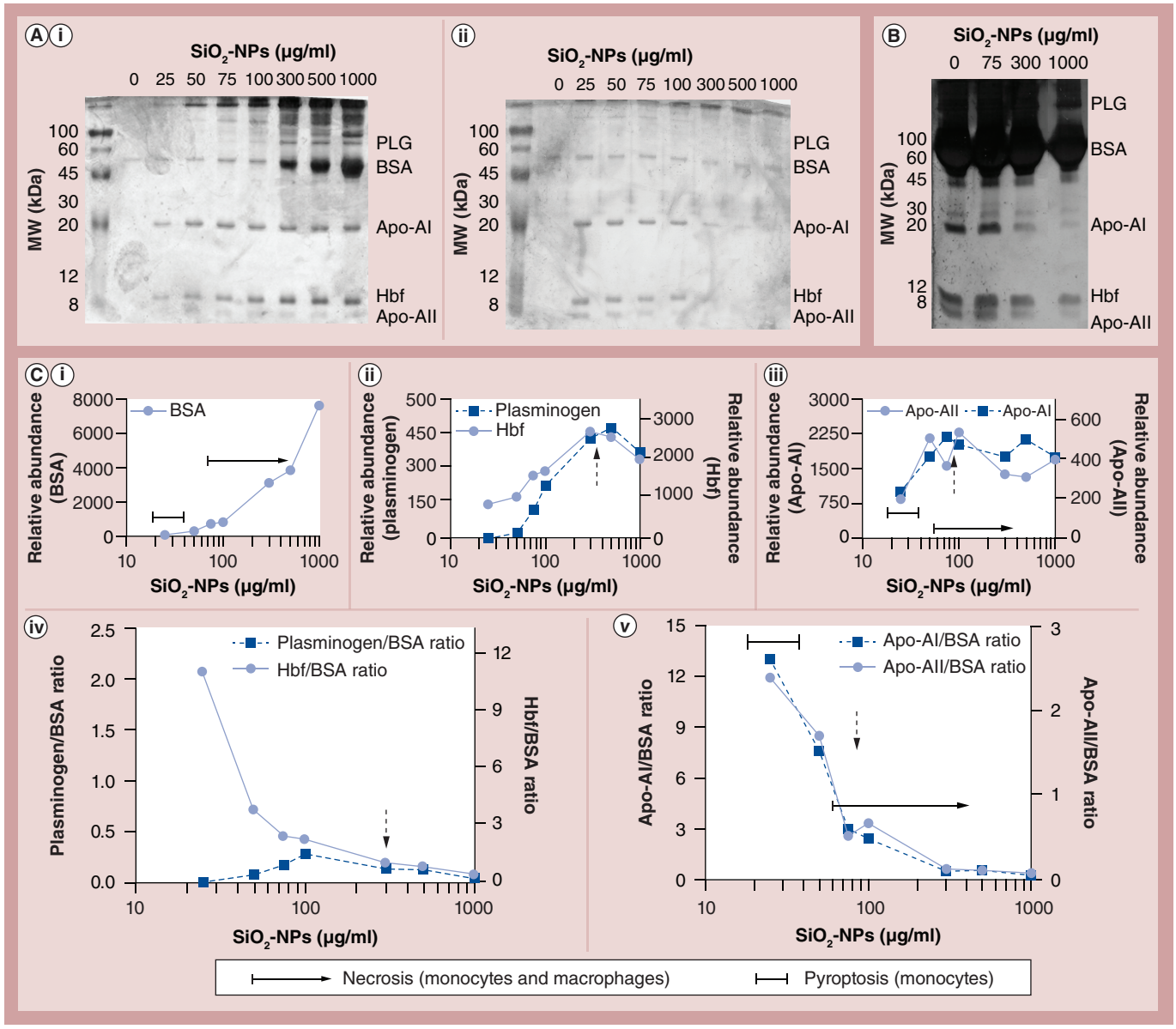

Figure 3. Fetal calf serum proteins bound to amorphous silica nanoparticles. (A) Ludox® TM-40 SiO_2-NPs (Sigma-Aldrich, MO, USA) were incubated for 15 min at 37°C in cell culture medium plus 10% fetal calf serum, washed and analyzed by SDS-PAGE (12%). **(A,i)** Equal sample volumes or **(A,ii)** equal sample amounts were loaded onto an SDS-PAGE and stained by silver nitrate. **(B)** Serum protein pattern determined by SDS-PAGE after incubation as above with SiO_2-NPs at the indicated doses and their elimination by ultracentrifugation. The bands corresponding to tandem mass spectrometry analysis-identified proteins (see Table 2) are indicated in both gels. **(A & B)** The values running down the left-hand side of each image indicate the MW in KDa of the molecular weight standard polypeptides used in the gel. **(C)** Quantification by densitometry of the proteins **(C,i)** BSA, **(C,ii)** plasminogen and Hbf and **(C,iii)** Apo-AI and Apo-AII identified by tandem mass spectrometry analysis, and **(C,iv and C,v)** their ratios compared with BSA. Dashed arrows point to SiO_2-NP concentrations corresponding to the saturation of protein binding. SiO_2-NP concentration ranges leading either to pyroptosis (monocytes) or to necrosis (both cells) are shown.
BSA: Bovine serum albumin; Hbf: Fetal bovine hemoglobin (β subunit); PLG: Plasminogen; SiO_2-NP: Amorphous silica nanoparticle.

Characterization of SiO_2-NP cytotoxicity on monocytes & macrophages in FCS

The induction of IL-1β release by SiO_2-NPs from both monocytes and macrophages involves the activation of caspase-1 via a mechanism requiring endosomal acidification also in serum (Figure 2A & Supplementary Figure S2B). On the contrary, cytotoxicity is substantially decreased in serum and shows different kinetic features, cell-type specificities and inhibitor sensitivities (Figures 2B & 2C). First, while in media lacking serum the cell death induced by SiO_2-NPs is relatively rapid, in the presence of serum it is a two-phase process, characterized by an initial fast drop of the mitochondrial metabolism and a subsequent

Table 2. Fetal calf serum proteins bound to amorphous silica nanoparticle surface identified by tandem mass spectrometry analysis.

Spot	Accession number[†]	Protein name	Theoretical mass (Da)[‡]	Score[§]	Peptides[¶]	Sequence coverage
PLG	P06868	Plasminogen	88,393	1798/47	35 (23)	51
BSA	P02769	Serum albumin	66,432	4441/46	43 (28)	67
Apo-AI	P15497	Apo-AI	27,549	4630/46	26 (15)	72
Hbf	P02081	Fetal hemoglobin β subunit	15,859	454/47	10 (5)	63
Apo-AII	P81644	Apo-AII	8722	741/46	6 (3)	55

[†]Identification of protein with the highest score from analysis of quantitative TOF data using in-house MASCOT. All files were searched against the SwissProt database_2011_05 (528,048 total sequences).
[‡]Values refer to the mature (secreted) proteins and were determined using ProtParam.
[§]MASCOT protein score/ion score identity threshold ($p < 0.05$).
[¶]Number of peptide sequences matched; significant matches are shown in brackets ($p < 0.05$).
BSA: Bovine serum albumin; PLG: Plasminogen.

slowly occurring cell lysis. EC50% values for the MTS assay are approximately 75 µg/ml for both of the cell lines after a 4-h incubation, and decrease to 65 and 25 µg/ml, respectively, for macrophages and monocytes after a 20-h incubation. The lactate dehydrogenase release assay, checking cellular membrane rupture, yields very high EC50% values (above the concentration interval evaluated) after a 4-h incubation, with values of approximately 70 and 25 µg/ml for macrophages and monocytes, respectively, after a 20-h incubation. In serum, monocyte viability is affected by SiO_2-NPs more slowly than macrophage viability, as they require longer incubation times to reach their maximal values. However, considering their lower NP-capturing efficacy [1], monocyte sensitivity to SiO_2-NPs is higher than that of macrophages.

Remarkably, at doses below 75 µg/ml, the inhibition of endosomal acidification and of caspase-1 substantially blocked the slowly occurring (20-h) NP toxicity in monocytes, but had negligible or weaker protective effects on macrophages (Figures 2B & 2C). On the contrary, at SiO_2-NP doses above the 75 µg/ml threshold, both macrophage and monocyte death is insensitive to Ac-YVAD-CMK and BafA1. In agreement, the membrane-disrupting activity of NPs is inhibited by serum and only appears at high NP concentrations (Figure 1C).

The differential involvement of caspase-1 in monocyte death induced by SiO_2-NPs in the smaller dose range, after a prolonged incubation, is also supported by the effect of oxidized ATP. This inhibitor prevents the ATP-dependent activation of caspase-1 after binding to P2X7 receptors on monocytes and macrophages [36–39], likely to occur due to the strong release of ATP in the extracellular medium of both cells in correspondence with cellular lysis (Supplementary Figure S4). Oxidized ATP significantly downregulated IL-1β production induced by SiO_2-NPs in both monocytes and macrophages (Figure 2A), but only reduced the delayed death induced by SiO_2-NPs in monocytes (Figure 2C).

In Supplementary Figure S5, we show that Ac-YVAD-CMK and BafA1 did not significantly modify the association of NPs with both monocytes and macrophages. We found that these inhibitors also reduced TNF-α and (less strongly) IL-6 secretion induced by SiO_2-NPs in monocytes and macrophages both in the absence or presence of serum (Supplementary Figure S6). This suggests that the specific pathway leading to the secretion of cytokines different from IL-1β activated by SiO_2-NPs may also be positively modulated by endosomal acidification and caspase-1. However, we showed that the stimulation of cytokine production by the Toll-like receptor 4 agonist lipopolysaccharide (LPS), which is independent of endolysosomal acidification, is poorly inhibited by BafAI and selectively blocked by Ac-YVAD-CMK (Supplementary Figure S7). Eventually, we proved that SiO_2-NPs indeed induce the activation of caspase-1 in both monocytes and macrophages, as evidenced by the formation of the mature caspase-1 20-kDa fragment and by the caspase-1-dependent processing of pro-IL-1β into the mature form, in serum and in no serum (Supplementary Figure S8). In addition, we showed that SiO_2-NPs can induce the transcription of the pro-IL-1β gene (Supplementary Figure S9) and that LPS, the main microbial costimulant of cytokine production, suggested to synergize with SiO_2-NPs [11], increased the synthesis of pro-IL-1β but did not improve that of caspase-1 (Supplementary Figure S8). Therefore, LPS, while able to strongly improve mature IL-1β release induced by SiO_2-NPs, had no effect on monocyte and macrophage sensitivity to the cytotoxic effects of SiO_2-NPs (Supplementary Figure S10), since it acts prevalently

10.2217/NNM.14.22

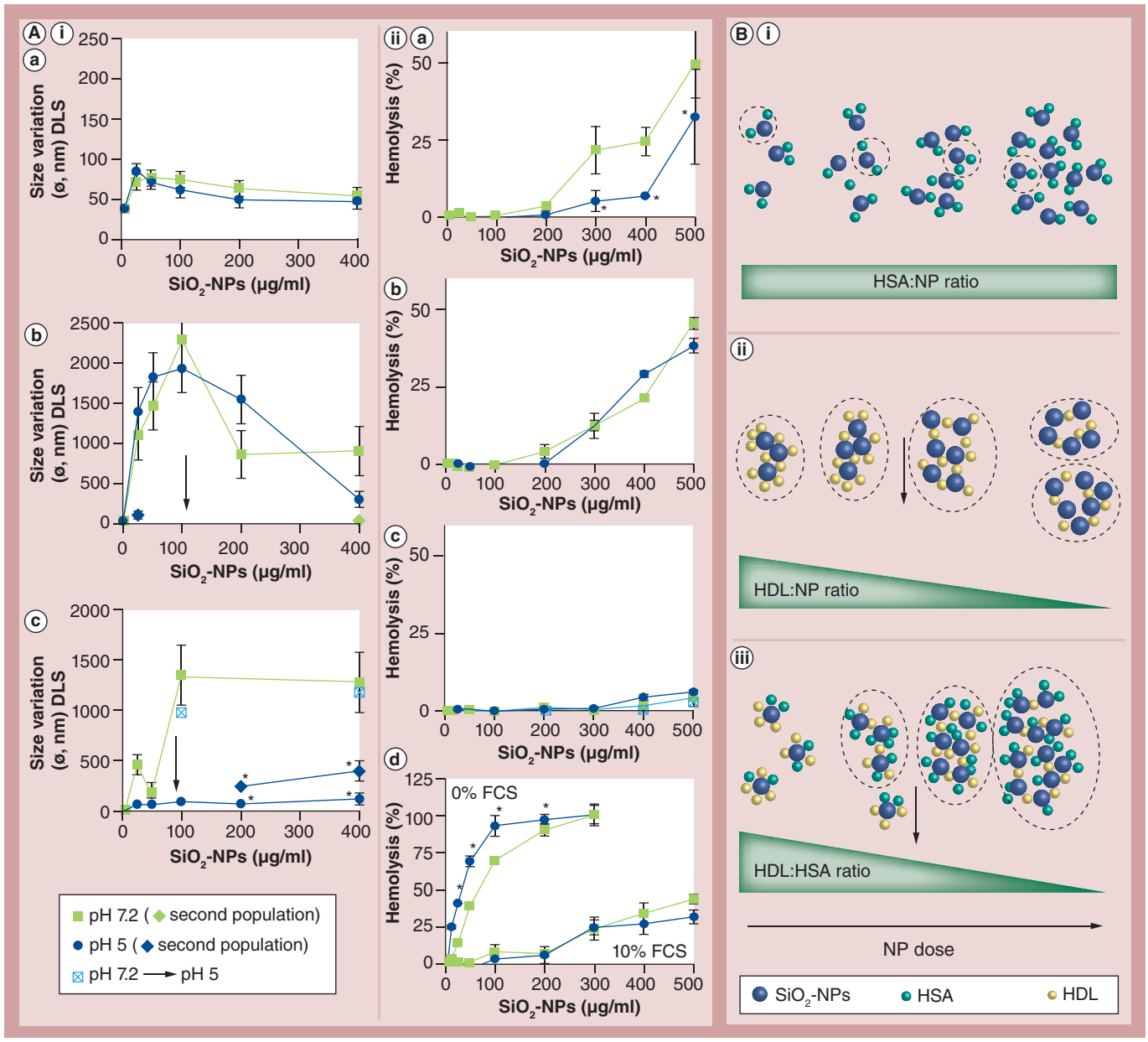

Figure 4. Effect of human high-density lipoproteins and human serum albumin on the aggregation state and hemolytic efficacy of amorphous silica nanoparticles and their modulation by endosomal-like acidic pH. (A,i) Volume-weighted DLS distribution analyses of Ludox® TM-40 SiO_2-NPs (Sigma-Aldrich, MO, USA) incubated for 10 min at 37°C with **(A,i,a)** HSA 5 mg/ml, **(A,i,b)** HDL 35 µg/ml or **(A,i,c)** both HDL and HSA, in phophate-buffered saline plus citrate 5 mM at pH 7.2, 5 or 7.2 (10-min preincubation) then lowered to pH 5. The circles represent the main distribution, while the diamonds represent the second distribution (20–40% of the main distribution). **(A,ii)** Red blood cells lysis induced by SiO_2-NPs at 37°C for 20 h in **(A,ii,a)** HSA 5 mg/ml, **(A,ii,b)** HDL 35 µg/ml or **(A,ii,c)** both HDL and HSA. **(A,ii,d)** Red blood cell lysis (%) with or without 10% FCS at pH 5 and 7.2. Data represent the means ± standard error of the mean (n = 3). The arrows indicate the SiO_2-NP dose corresponding to the saturation of HDL recruitment in the corona. **(B)** The effect of HSA, HDL and of both HSA and HDL on the dispersion/aggregation of SiO_2-NPs as a function of the NP dose, deduced by DLS data. Dashed circles delimit the NP/protein agglomerates formed in different conditions, and arrows point to the NP dose that leads to the recruitment of all HDL present in the medium on NPs. **(B,i)** In HSA only, upon NP increase in solution, the surface concentration of HSA on NPs (HSA:NP ratio) is constant, due to high availability of this protein in 10% serum, and NP/HSA complexes are small and monodispersed. **(B,ii)** In HDLs only, high NP crosslinking is effectively obtained due to the ability of less concentrated HDL in 10% serum to bind more than one NP. This leads to the agglomeration of NPs. **(B,iii)** In both HDL and HSA, a full corona forms around small monodispersed NPs at low nanoparticle dose (before the arrow), while in conditions of growing HDL shortage (indicated by the green triangle marked as HDL:HSA ratio), big protein–NP aggregates are formed.
*Indicates all cases in which the effect of SiO_2-NPs at acidic pH is significantly different ($p < 0.05$) from that at neutral pH.
DLS: Dynamic light scattering; FCS: Fetal calf serum; HDL: High-density lipoprotein; HSA: Human serum albumin; NP: Nanoparticle; SiO_2-NP: Amorphous silica nanoparticle.

by increasing the synthesis of the precursor pro-IL-1β, and not on the level of caspase-1.

Serum proteins adsorbed on SiO_2-NPs

To elucidate the possible role of specific serum factors, we investigated the pattern of the proteins associated with the NPs in the conditions of cellular assays. NPs were incubated with 10% FCS (pH 7.2), collected by centrifugation and, after extensive washings, the stably adsorbed proteins were separated by SDS-PAGE and identified by LS MS/MS (Figure 3A & Table 2). HDL-associated Apo A-I and Apo A-II are the main proteins bound to the NPs at concentrations below 75–100 µg/ml, while fetal bovine hemoglobin is more variably present depending on serum batch (data not shown). The analysis of the SiO_2-NP supernatant after centrifugation suggests that the observed change of the composition of NP-associated proteins above 75 µg/ml NP concentration in 10% FCS is due to the shortage of available HDL, in agreement with their relatively small concentration in serum compared with bovine serum albumin (BSA) (Figure 3B). Apo-AI and Apo-AII reach a plateau at approximately 100 µg/ml, while plasminogen and fetal hemoglobin reach a plateau at approximately 300 µg/ml (Figure 3C). At NP concentrations ≥75–100 µg/ml, BSA, and in smaller amounts plasminogen, become predominantly associated with NPs. This phenomenon determines a characteristic decrease of the HDL/BSA ratio upon increasing the NP concentration, particularly evident when free HDL is lacking in solution, (i.e., above 75–100 µg/ml NPs).

Modulation of the aggregation state & membranolytic action of SiO_2-NPs by HDL & HSA

NPs are known to form nanoaggregates with proteins in a dose-dependent way, influencing their interaction with cells [40–45]. We have already shown that in 10% FCS SiO_2-NPs have a relatively stable corona and are poorly aggregated up to 100 µg/ml, while, for higher NP concentrations, they form large aggregates with serum proteins [1]. In the previous paragraph, we showed that indeed this critical dose of SiO_2-NPs in 10% FCS corresponds to the maximal binding of available HDL in solution, and that above this value BSA progressively predominates in the corona. We therefore focus our attention on human HDL and HSA, analyzing their proaggregative and membrane-damaging actions, when tested separately or in combination. To analyze if HDL and HSA could account for the effects we observed in FCS, we chose protein concentrations resembling those of the equivalent bovine proteins in 10% FCS [46]. Since BSA is more concentrated than HDL in FCS (~50 mg/ml and ~350 µg/ml, respectively) we used the doses of 5 mg/ml and 35 µg/ml, respectively. At pH 7.2, the dynamic light scattering measurement (Figure 4) showed that HSA alone (5 mg/ml) forms a stable corona on the NPs in the whole concentration range explored (20–400 µg/ml), preventing NP aggregation. On the contrary, HDL alone (35 µg protein/ml) induced large polydisperse aggregates (diameters ~1–2.5 µm) at all NP doses, strongly suggesting the formation of HDL protein bridges between NPs, while HSA used at a dose

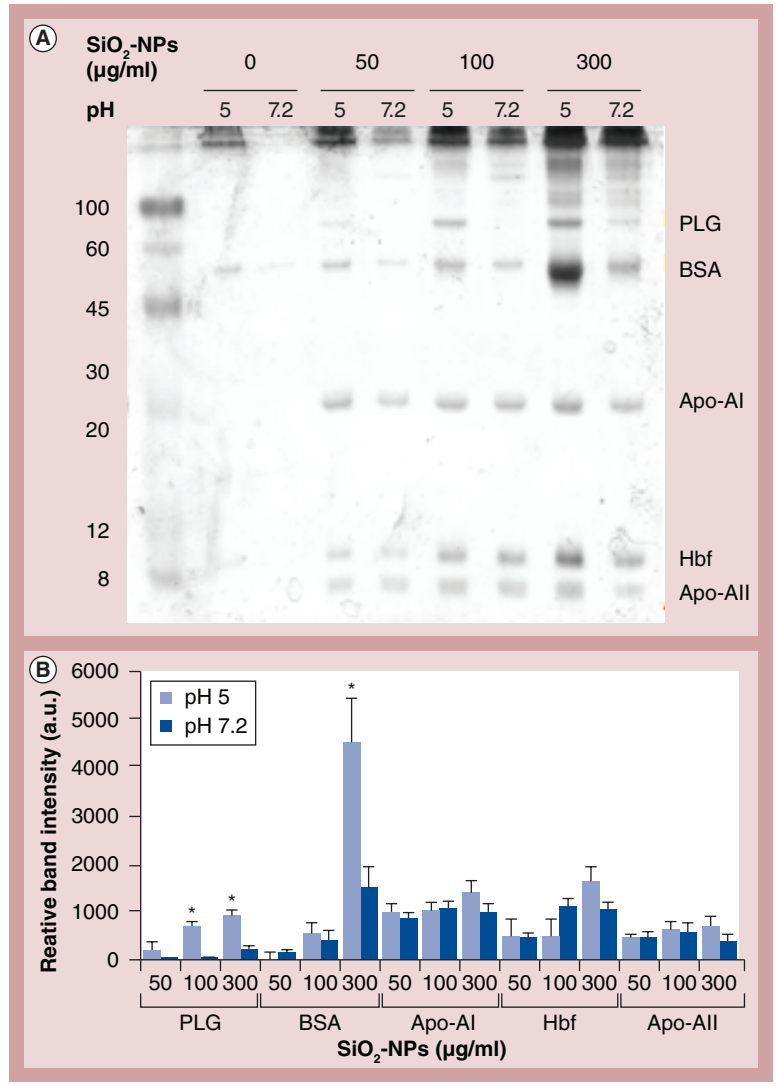

Figure 5. Effect of endosomal-like acidic pH on the composition of the amorphous silica nanoparticles' serum corona. (A) SDS-PAGE of the protein corona of Ludox® TM-40 SiO_2-NPs (Sigma-Aldrich, MO, USA) after incubation (37°C, 15 min) in 10% fetal calf serum as indicated. **(A)** The values running down the left-hand side of the image indicate the MW in KDa of the molecular weight standard polypeptides used in the gel. **(B)** Proteins identified by tandem mass spectrometry analysis are indicated and quantified by densitometry. Data are the means ± standard error of the mean (n = 3).
*$p < 0.05$ versus pH 7.2.
BSA: Bovine serum albumin; Hbf: Fetal bovine hemoglobin (β subunit); PLG: Plasminogen; SiO_2-NP: Amorphous silica nanoparticle.

10.2217/NNM.14.22

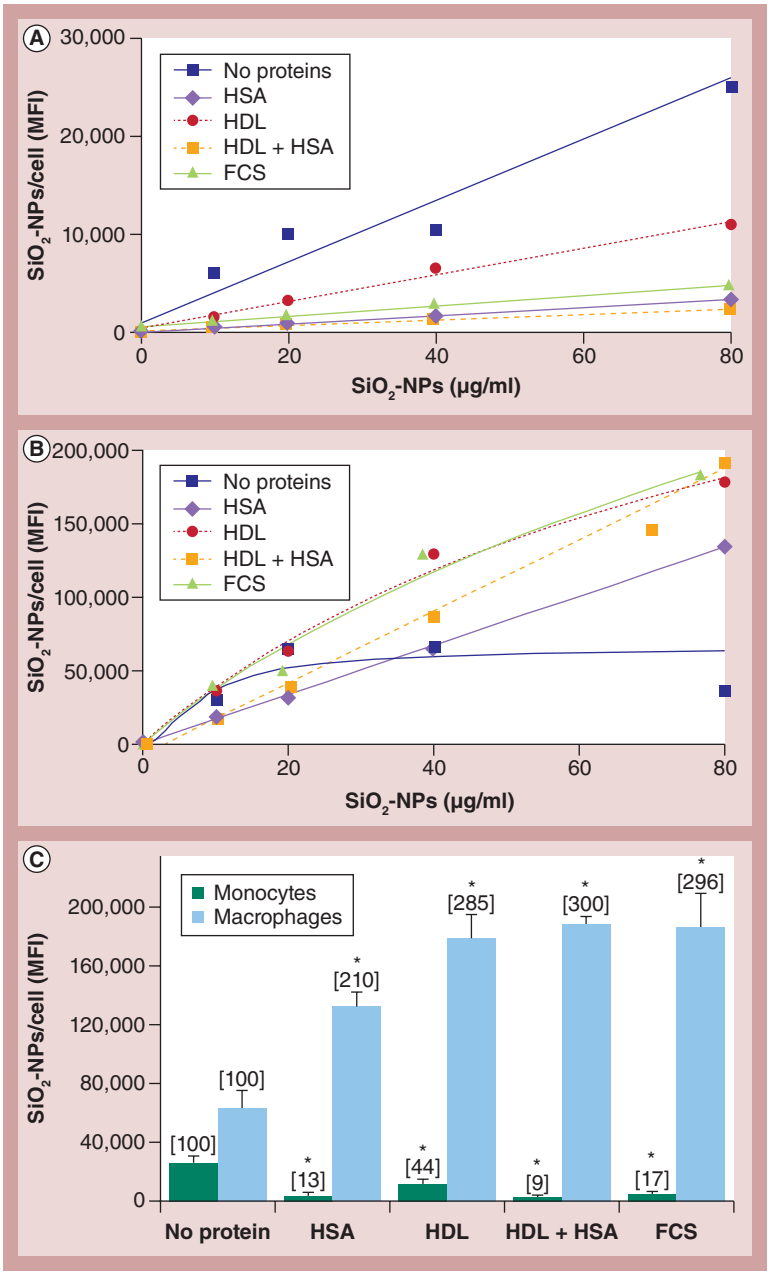

Figure 6. Effect of human serum albumin and high-density lipoproteins on amorphous silica nanoparticle cellular association. (A) Monocytes and **(B)** macrophages were incubated at 37°C for 20 h with fluorescein isothiocyanate-labeled Stöber SiO_2-NPs in culture medium containing no protein, 10% FCS, HDL 35 µg/ml, HSA 5 mg/ml and both HDL and HSA, and analyzed by flow cytofluorimetry to measure nanoparticle-associated fluorescence. Representative binding curves are shown, obtained by nonlinear fitting of data points obtained from duplicates. **(C)** SiO_2-NP association with monocytes and macrophages in the indicated conditions (SiO_2-NP dose: 80 µg/ml). Data are mean ± standard error of the mean (n = 3). Values in square brackets indicate cell association expressed as percentage of that observed in the absence of protein.
*Indicates statistically significant difference ($p < 0.05$).
HDL: High-density lipoprotein; HSA: Human serum albumin; FCS: Fetal calf serum; MFI: Mean fluorescence intensity; SiO_2-NP: Amorphous silica nanoparticle.

comparable with HDL (35 µg/ml) at pH 7.0 was still unable to aggregate NPs (Supplementary Figure S11). Interestingly, the simultaneous presence of HDL and HSA, mimicking the serum condition, mitigates the formation of NP agglomerates (80–300 nm diameter range) at NP doses below 100 µg/ml but cannot prevent the formation of microaggregates (~1200 µM) above this threshold, similarly to what was observed in FCS [1].

At endosomal-like pH 5, the behavior of separate HSA and HDL is similar to that observed at pH 7.2, but NP incubation with both proteins determined the formation of dispersed NPs with a diameter of approximately 100 nm, indicative of the presence of corona-coated dispersed NPs. However, decreasing the pH from 7.2 to 5 after the formation of NP aggregates in the presence of HSA/HDL, a protocol simulating the pH shift experienced by the NP–protein aggregates formed in the neutral extracellular medium and then internalized in acidic endosomes, did not change their size. Monodispersed NPs with a corona made of HSA alone show a strong membranolytic activity above a threshold of 100 µg/ml, while large aggregates formed by HDL and NPs are effective above 200 µg/ml. Notably, the hemolytic activity of NPs in the presence of both HDL and HSA was substantially reduced and detectable only above 100 µg/ml, a situation which is reminiscent of that occurring in 10% FCS. In acidic conditions, the hemolytic power of SiO_2-NPs in the presence of all serum proteins was slightly reduced, while significantly improved in the absence of proteins. This is consistent with the fact that acidic pH scarcely alters the protein composition of serum corona with the only exception of BSA, whose amount increases threefold at pH 5 compared with pH 7.2 (Figure 5).

HDL and HSA influence monocyte/macrophage SiO_2-NP binding, endocytosis and cytotoxicity. We have shown that HDL and HSA account for the dispersion/aggregation of SiO_2-NPs and for their decreased membranolytic effects in serum. We then analyzed the effect of these proteins on cell association and endocytosis. As already known [1], the amount of NPs taken up by macrophages was much higher than that by monocytes (Figure 6) in all conditions. Moreover, while uptake of SiO_2-NPs by monocytes linearly increased with the NP dose, uptake of SiO_2-NPs by macrophages followed a saturation dose–response profile. Both tested proteins reduced NP uptake by monocytes, with HSA more effective (~50% reduction for HDL and ~90% for HSA). On the contrary, they increased the capture of NPs by macrophages, with HDL more effective (~300% increase for HDL and ~200% increase for HSA) compared with the no-serum condition. Coincubation of NPs with HDL and HSA maintained the decreased or increased uptake levels

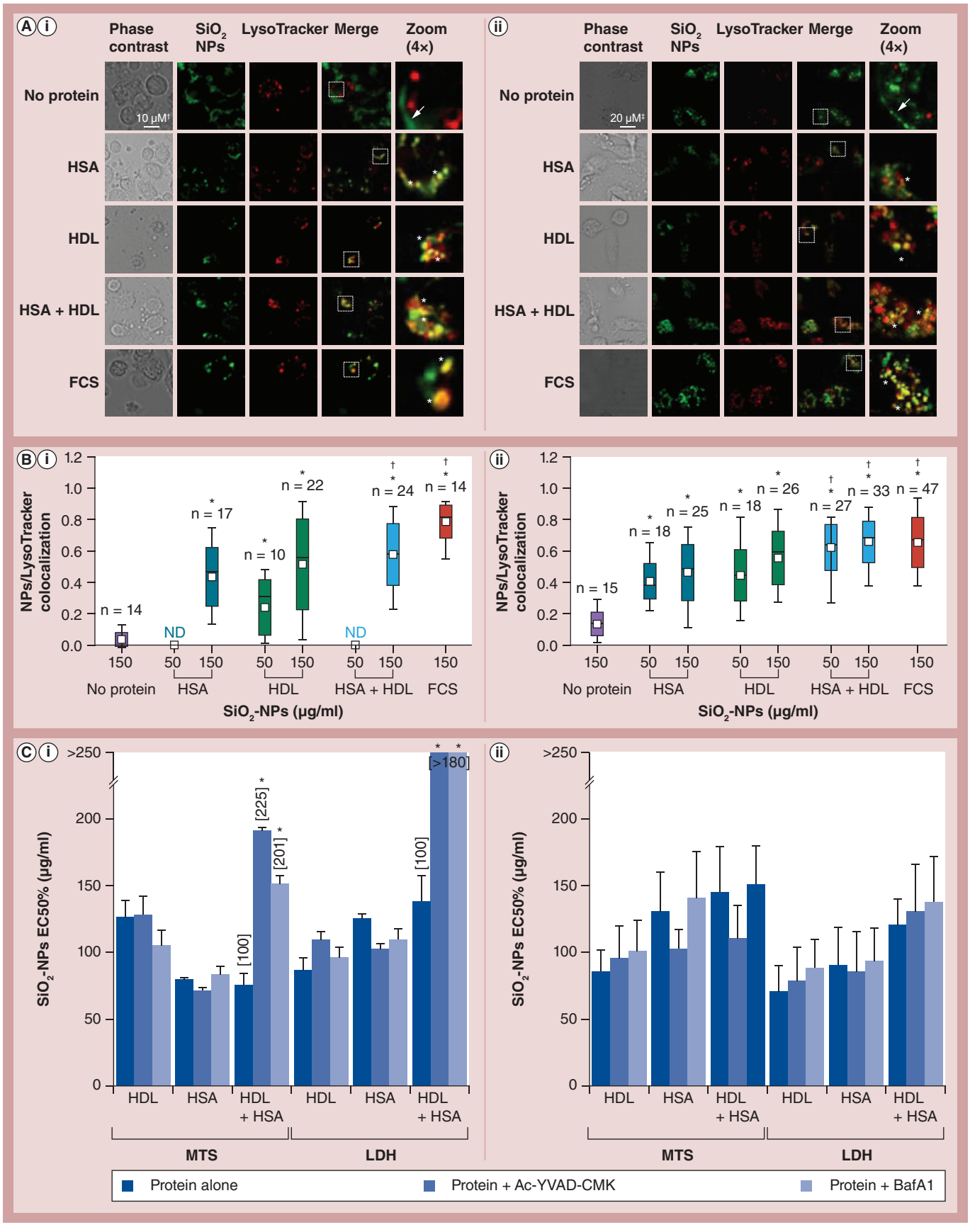

10.2217/NNM.14.22

Figure 7. Effect of human serum albumin and high-density lipoproteins on the transport of amorphous silica nanoparticles to acidic endolysosomes in monocytes and macrophages and on the nanoparticle cytotoxic efficacy in the same cells (cont.; see previous page). (A) Confocal images of **(A,i)** monocytes and **(A,ii)** macrophages treated at 37°C for 1.5 h with 150 µg/ml Stöber SiO_2-NPs (in medium with HSA 5 mg/ml and HDL 35 µg/ml), stained with LysoTracker Red. The fields in the dotted squares are enlarged 4×. The arrows point to the plasma membrane, and asterisks indicate SiO_2-NP/acidic compartments colocalization. Controls without nanoparticles (just LysoTracker) are shown in Supplementary Figure S12. **(B)** NP/LysoTracker colocalization after incubation as above estimated using Image J software and expressed as Pearson's (Rr) correlation coefficient (1 = 100% colocalization; 0 or less = no colocalization). The bars are the range, the boxes are the standard deviation, the small white squares are the mean and the lines in the boxes are the mode. *Indicates $p < 0.05$ versus no protein; †indicates $p < 0.05$ versus corresponding HSA values. **(C)** SiO_2-NP effect concentration (50%; EC50%) values resulting from cytotoxicity curves (MTS and LDH assays) exemplified in Supplementary Figure S3B, after treatment of **(C,i)** monocytes and **(C,ii)** macrophages at 37°C for 20 h with Ludox® TM-40 SiO_2-NPs (Sigma-Aldrich, MO, USA) in medium plus HDL 35 µg/ml, HSA 5 mg/ml or HDL plus HSA with no inhibitors, or in the presence of Ac-YVAD-CMK 200 µM and BafAI 12.5 nM (1-h preincubation). Data are the means ± standard error of the mean (n = 3). The values in square brackets are EC50 expressed as the percentage of that observed in the absence of inhibitors. *Indicates that the difference is significant ($p < 0.05$ vs proteins alone).
†The scale bar is the same for all images in **(A,i)**.
‡The scale bar is the same for all images in **(A,ii)**.
Ac-YVAD-CMK: *N*-acetyl-tyrosyl-valyl-alanyl-aspartyl chloromethyl ketone; EC50%: SiO_2-NP dose resulting in half-maximal effect; HDL: High-density lipoprotein; HSA: Human serum albumin; FCS: Fetal calf serum; LDH: Lactate dehydrogenase; MTS: 3-(4,5-dimethylthiazol-2-yl)-5-(3-carboxymethoxyphenyl)-2-(4-sulfophenyl)-2H-tetrazolium; ND: Not determined due to low signal; SiO_2-NP: Amorphous silica nanoparticle.

observed for the most efficient proteins and mimicked the effect of 10% FCS.

Confocal microscopy analysis (Figures 7A & 7B) showed that the combination of HDL and HSA determined a localization of SiO_2-NPs in acidic endolysosomal compartments significantly more efficiently than the one induced by HSA and HDL alone, and closely approaching the almost-total colocalization induced by 10% serum. SiO_2-NPs induced a caspase-1/V-ATPase-dependent cell death of monocytes but not of macrophages when incubation was carried out in the presence of both HDL and HSA, while a caspase-1/V-ATPase-independent one in both cell types in the presence of HDL or HSA (Figure 7C).

Discussion

Recent evidence indicates that amorphous SiO_2, although used in industry as a food additive and as a platform for nanotheranostics, may determine toxicological effects. Monocytes and macrophages are known to be especially sensitive to the cytotoxic/proinflammatory effects induced by amorphous SiO_2-NPs. Moreover, considering their lower NP-capturing efficacy, monocytes are intrinsically more susceptible than macrophages to the effects of SiO_2-NPs.

Here, we show that in no serum, SiO_2-NPs determined a caspase-1/V-ATPase-independent rapid cell lysis in both monocytes and macrophages, in agreement with the enrichment of cytosolic proteins in the corona of SiO_2-NPs incubated with epithelial A549 cells in no serum [19]. However, while serum proteins apparently shield the membrane-active surface silanols, inhibiting their known bilayer-destabilizing action and acute toxicity [47,48], they determined other specific effects.

SiO_2-NPs still induce a rapid, caspase-1/V-ATPase-insensitive necrosis in both cell types at high doses in serum, but induced pyroptosis at lower doses after a longer time in monocytes only. Such a delayed caspase-1/V-ATPase-dependent death apparently renders monocytes more sensitive to SiO_2-NPs than macrophages.

The prevalence of HDL in the corona below 75 µg/ml NPs or of BSA above this critical concentration suggested a differential modulatory role of these two serum proteins. Indeed, purified human HDL at doses similar to those present in 10% FCS induce a strong particle aggregation, mimic the binding behavior of SiO_2-NPs in the presence of FCS to monocytes and macrophages and the serum-induced internalization in acidic endosomes. Moreover, the presence of HDL determined a protective effect similar to that of FCS on the toxicity of nude SiO_2-NPs. Purified HSA alone prevents particle aggregation, appears more efficient in reducing cell binding and still induces, although to a lesser extent compared with HDL, endolysosomal localization, and has a protective effect. Interestingly, NPs with a corona formed only by HDL or HSA induce a caspase-1/V-ATPase-insensitive cell death, while pyroptosis emerges only when the two proteins are combined in the corona. The simultaneous presence of the two proteins also leads to a better mimicking of the SiO_2-NP cell association, intracellular localization and aggregation properties in FCS. The functional importance of serum lipoproteins in NP–cell interactions, suggested by our study, is consistent with their presence in the corona of several NPs [15,19,40,44,45,49–51].

Based on our data, we formulate the model depicted in Figure 8. The central idea is that relatively small SiO_2-NP/serum protein complexes (<300 nm), equipped with a HDL-enriched corona, although unable to directly destabilize the cell plasma membrane,

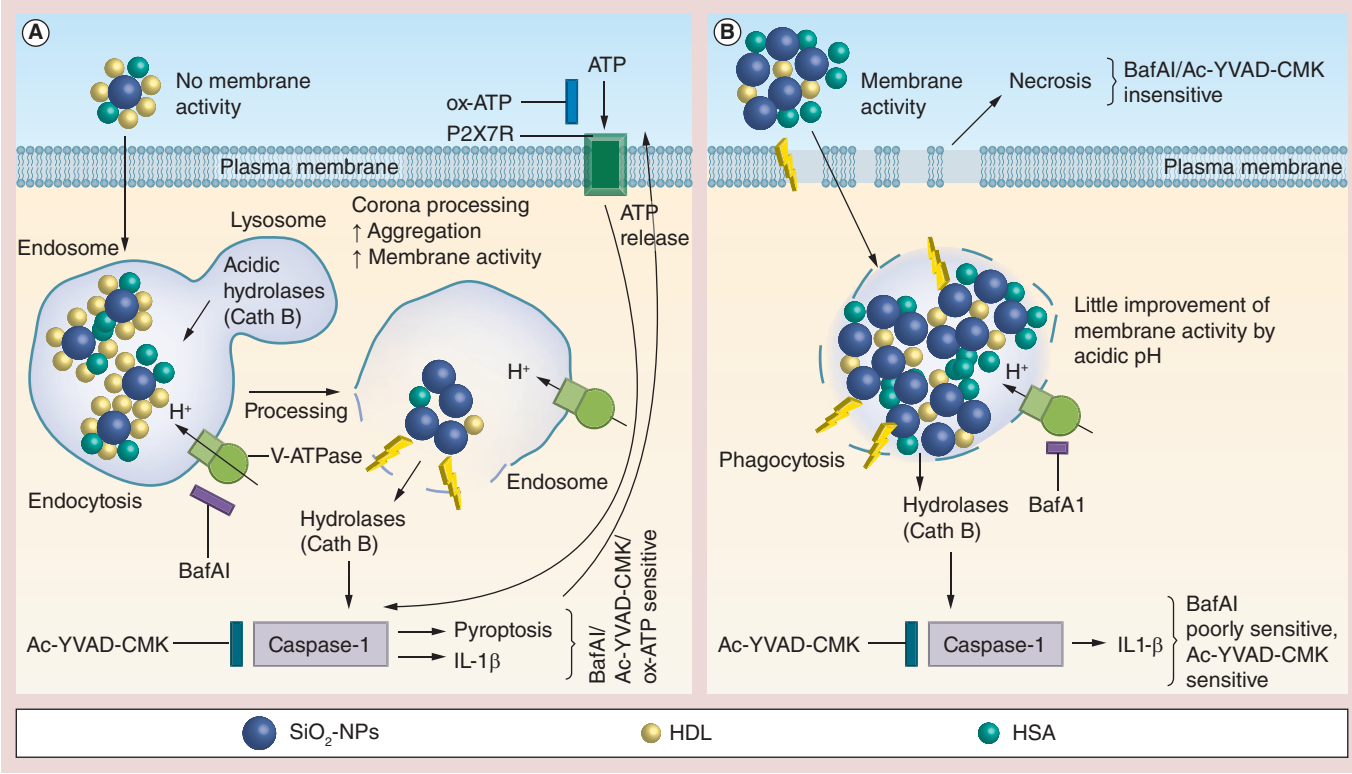

Figure 8. Cytotoxic/proinflammatory mechanisms induced in monocytes and macrophages by amorphous silica nanoparticles in serum as a function of the high-density lipoproteins:human serum albumin ratio. (A) Cytotoxic effect of poorly aggregated SiO_2-NPs in monocytes only with a corona enriched in HDL (high HDL:HSA ratio; formed below the 75 µg/ml threshold in 10% fetal calf serum), devoid of membrane-damaging power. The cellular effects of NPs follow internalization and require acidification and caspase-1 to trigger both IL-1β production and cell pyroptosis. Notice the possible role of acidic hydrolases in re-exposing silanol membrane active moieties in acidic endosomes. ATP released in the extracellular medium is shown to positively synergize caspase-1 activation. **(B)** Cytotoxic action of large aggregates formed by NPs in conditions of defective HDL in the corona (low HDL:HSA ratio; formed above the 75 µg/ml threshold in both monocytes and macrophages), endowed with membrane-damaging effects. At these NP concentrations, in 10% fetal calf serum, some serum proteins are indeed depleted from the solution by the NPs, and HDL in particular. Like nude NPs (see Figure 1D), NP–protein agglomerates may affect the plasma membrane, due to the partial exposure of silanols. Their cytotoxic action is less dependent on intracellular acidification and on caspase-1 activity. The sites of BafAI (vacuolar-type H^+-ATPase), Ac-YVAD-CMK (caspase-1) and ox-ATP (P2X7 receptor) actions are indicated. The lightning bolt symbols indicate the damage/disruption of the lipid bilayer of membranes.
Ac-YVAD-CMK: *N*-acetyl-tyrosyl-valyl-alanyl-aspartyl chloromethyl ketone; BafAI: Bafilomycin AI; Cath B: Cathepsin B; HDL: High-density lipoprotein; HSA: Human serum albumin; NP: Nanoparticle; ox-ATP: Oxidized ATP; SiO_2-NP: Amorphous silica nanoparticle; V-ATPase: Vacuolar-type H^+-ATPase.

unlike bare NPs, can be activated by endolysosomal acidic pH after internalization (Figure 8A). Since we showed that acidic pH does not disassemble the protein corona and, consistently, does not improve the NP membrane-disrupting efficacy in serum, we suggest that the digestion/processing of NP-adsorbed proteins by lysosomal acidic hydrolases may re-expose the membrane-destabilizing silanols. This would eventually lead to caspase-1 activation, IL-1β secretion and cell lysis by pyroptosis. In the proposed scheme, we also present the synergistic loop due to the release of cytosolic ATP after cell lysis. ATP may act on bystander cells, partially contributing to the activation of caspase-1 by binding to ectopic receptors.

In agreement with our data, Wang and coworkers showed that polystyrene particles directly permeabilize the plasma membrane of epithelial cells in no serum, while they enter with their protein corona in acidic endosomes in the presence of serum [52]. Here, their surface is later re-exposed by proteolytic cleavage and determines cell death by lysosomal destabilization. In addition, in our study, we provide evidence that that big SiO_2-NP/serum protein clusters (>1000 nm), formed in conditions in which critical serum proteins are defective and characterized by a predominance of albumin over HDL, may also directly damage the cell plasma membrane (Figure 8B). This ability may be due to the lower affinity of albumin for the silica surface compared with HDL and/or to the partial exposure of the membrane-active silica surface.

Notably, caspase-1/V-ATPase-dependent cell death triggered by SiO_2-NPs coated with HDL:HSA (high

10.2217/NNM.14.22

ratio) was absent or not relevant in macrophages, possibly due to the downregulation of the caspase-1 activator protein pyrin accompanying the differentiation of human monocytes into macrophages [53]. This points to the importance of using human primary cells with different phenotypes to unravel the NP corona functions. In fact, although the corona proteins are known to negatively affect the cellular binding of NPs [1,19,54], here we reveal that specific corona proteins induce diverse cytotoxic effects in closely related human phagocytic cells. In particular, we support the possibility that plasma lipoproteins, and especially HDL, play a critical role in modulating NP bioactivities [15,44,45,50].

FCS, although relevant for *in vitro* cellular studies, lacks the complement and coagulation systems [55], and has peculiar composition differences with respect to the human plasma [19,49,56]. Nevertheless, the higher prevalence of HDL in human plasma compared with FCS [46] suggests that these lipoproteins may play an even stronger modulatory role on SiO_2-NPs also *in vivo*. Additional investigations dedicated to the human plasma-derived SiO_2-NP corona are necessary to define the real incidence of specific proteins in conditions closer to the *in vivo* situation.

Future perspective

Future studies will be oriented to identify the full array of specific human plasma components involved in the modulation of NPs, and to ascertain the reciprocal influence/interference of the various corona components at different NP doses on the different functions of relevant human cell types. This information will be strategic to design safe nanotheranostics. Finally, understanding the physicochemical features of environmental, anthropogenic nanomaterials mediating this or similar interactions with specific host fluid biomolecules may be essential to fully understand their toxicological properties.

Executive summary

Amorphous silica nanoparticles induce differential cytotoxic/proinflammatory effects in monocytes and macrophages in the presence of serum but not in the absence of serum

- The action of amorphous silica nanoparticles (SiO_2-NPs) on human monocytes/macrophages is substantially different in the absence and in the presence of serum because specific serum proteins recruited in the corona change their cellular interactions and, consequently, their cytotoxic and proinflammatory properties.
- In no serum, the reactive silanols on the SiO_2-NP surface trigger a rapid necrosis of both cells by damaging the cell plasma membrane.
- In 10% fetal calf serum, SiO_2-NPs induce a delayed lytic death of monocytes coupled with a strong IL-1β release, below the approximate dose of 75 µg/ml. This process required endolysosomal acidification and caspase-1, and resembled the features typical of pyroptosis.
- Both macrophages and monocytes incubated with fetal calf serum are subjected to fast cellular necrosis, not requiring endosomal acidification and caspase-1, above the approximately 75 µg/ml SiO_2-NP dose.

High-density lipoprotein and albumin are major corona components determining SiO_2-NP dispersion and the interaction with monocytes/macrophages

- The SiO_2-NP corona in 10% fetal calf serum is characterized by a high high-density lipoprotein (HDL):bovine serum albumin ratio below a critical concentration (75–100 µg/ml), separating the range of NP concentrations leading to pyroptosis in monocytes from that resulting in necrosis of both monocytes and macrophages, and by a low HDL:bovine serum albumin ratio above this value.
- Human HDL plus human serum albumin mimic the dose-dependent dispersion/aggregation state and the membrane-destabilizing efficacy of SiO_2-NPs in serum, and are responsible for the differential binding/endocytosis and proinflammatory/cytotoxic responses induced by these particles in monocytes and macrophages compared with the no-serum condition.
- A SiO_2-NP corona characterized by a high HDL:albumin ratio, formed in serum excess, is linked to the induction of an endolysosomal acidification and caspase-1-dependent death in monocytes.
- Nanoagglomerates endowed with a low HDL:albumin ratio, obtained in serum defect, induce a rapid and passive lysis of both monocytes and macrophages.

Conclusion

- Monocytes, although much less effective in capturing SiO_2-NP/HDL/human serum albumin complexes, are more sensitive than macrophages to the induction of an inflammatory death by SiO_2-NPs, due to pyroptosis.
- The cytotoxic and proinflammatory effects of SiO_2-NPs do not simply depend on their material properties but are, on the contrary, due to an entity formed by nanoparticles and specific serum proteins leading to emerging bioactivities.
- HDL is a major component of the SiO_2-NP corona in serum and plays a functional role in the differential cytotoxic and proinflammatory effects induced by these nanoparticles in human monocytes and macrophages.

Acknowledgements

The authors thank the Centro Trasfusionale of the Hospital of Padua (ULSS 16) for providing buffy coats. The authors also thank F Rastrelli for assistance with the nuclear magnetic resonance spectra and K Leone for ATP assays.

Financial & competing interests disclosure

This work was supported by the European Community's Seventh Framework Programme (FP7/2007–2013) under grant agreement no. 201031 NANOPHOTO, the University of Padova, Italy (Ex 60%, 2009–2013 and PRAT 2011) and the Italian Ministry of Research (FIRB 2011, RBAP114AMK RINAME). The Varian 400 SS-NMR spectrometer used was acquired by the University of Padova thanks to funding from the Fondazione CARIPARO (Progetti di Eccellenza 'Nano-Mode' 2010). The authors have no other relevant affiliations or financial involvement with any organization or entity with a financial interest in or financial conflict with the subject matter or materials discussed in the manuscript apart from those disclosed.

No writing assistance was utilized in the production of this manuscript.

References

Papers of special note have been highlighted as:

- • **of interest**
- •• **of considerable interest**

1 Fedeli C, Selvestrel F, Tavano R, Segat D, Mancin F, Papini E. Catastrophic inflammatory death of monocytes and macrophages by overtaking of a critical dose of endocytosed synthetic amorphous silica nanoparticles/serum protein complexes. *Nanomedicine (Lond.)* 8(7) 1101–1126 (2012).

2 Broz P, von Moltke J, Jones JW, Vance RE, Monack DM. Differential requirement for caspase-1 autoproteolysis in pathogen-induced cell death and cytokine processing. *Cell Host Microbe* 8(6), 471–483 (2010).

3 Miao EA, Rajan JV, Aderem A. Caspase-1-induced pyroptotic cell death. *Immunol. Rev.* 243(1), 206–214 (2011).

•• **Outlines the main features of lytic and inflammatory cell death supported by caspase-1, or pyropotosis.**

4 Shao W, Yeretssian G, Doiron K, Hussain SN, Saleh M. The caspase-1 digestome identifies the glycolysis pathway as a target during infection and septic shock. *J. Biol. Chem.* 282(50), 36321–36329 (2007).

• **A suggestive attempt to identify new caspase-1 substrates involved in pyroptosis.**

5 Martinon F, Mayor A, Tschopp J. The inflammasomes: guardians of the body. *Annu. Rev. Immunol.* 27, 229–265 (2009).

6 Bauernfeind F, Ablasser A, Bartok E *et al.* Inflammasomes: current understanding and open questions. *Cell. Mol. Life Sci.* 68(5), 765–783 (2011).

7 Morishige T, Yoshioka Y, Inakura H *et al.* The effect of surface modification of amorphous silica particles on NLRP3 inflammasome mediated IL-1beta production, ROS production and endosomal rupture. *Biomaterials* 31(26), 6833–6842 (2010).

• **Amorphous silica nanoparticles (NPs) with various surface features are shown to activate caspase-1.**

8 Meunier E, Coste A, Olagnier D *et al.* Double-walled carbon nanotubes trigger IL-1beta release in human monocytes through NLRP3 inflammasome activation. *Nanomedicine* 8(6), 987–995 (2012).

• **Shows the importance of inflammasome and caspase-1 activation in mediating the effects of nanofibers on monocytes.**

9 Lunov O, Syrovets T, Loos C *et al.* Differential uptake of functionalized polystyrene nanoparticles by human macrophages and a monocytic cell line. *ACS Nano.* 5(3), 1657–1669 (2011).

• **Demonstrates a functional diversity between monocytes and macrophages when facing NPs.**

10 Hornung V, Bauernfeind F, Halle A *et al.* Silica crystals and aluminum salts activate the NALP3 inflammasome through phagosomal destabilization. *Nat. Immunol.* 9(8), 847–856 (2008).

•• **Shows that different particulates, including crystalline silica, can activate caspase-1, and hence IL-1β maturation, by destabilizing the endosomal membranes.**

11 Sandberg WJ, Lag M, Holme JA *et al.* Comparison of non-crystalline silica nanoparticles in IL-1beta release from macrophages. *Part. Fibre Toxicol.* 9, 32 (2012).

12 Sharp FA, Ruane D, Claass B *et al.* Uptake of particulate vaccine adjuvants by dendritic cells activates the NALP3 inflammasome. *Proc. Natl Acad. Sci. USA* 106(3), 870–875 (2009).

13 Reisetter AC, Stebounova LV, Baltrusaitis J *et al.* Induction of inflammasome-dependent pyroptosis by carbon black nanoparticles. *J. Biol. Chem.* 286(24), 21844–21852 (2011).

•• **The first evidence concerning the induction of pyroptosis by an anthropogenic NP (carbon black), using a murine macrophagic cell line.**

14 Walkey CD, Chan WC. Understanding and controlling the interaction of nanomaterials with proteins in a physiological environment. *Chem. Soc. Rev.* 41(7), 2780–2799 (2012).

15 Aggarwal P, Hall JB, McLeland CB, Dobrovolskaia MA, McNeil SE. Nanoparticle interaction with plasma proteins as it relates to particle biodistribution, biocompatibility and therapeutic efficacy. *Adv. Drug Deliv. Rev.* 61(6), 428–437 (2009).

• **Emphasizes the general interaction of plasma proteins with virtually all nanostructures, and shows the quasi-omnipresence of lipoproteins and albumin in their coronas.**

16 Mortensen NP, Hurst GB, Wang W, Foster CM, Nallathamby PD, Retterer ST. Dynamic development of the protein corona on silica nanoparticles: composition and role in toxicity. *Nanoscale* 5(14), 6372–6380 (2013).

• **Focuses on the likely modulation of amorphous silica NP–cell interactions by the corona protein composition.**

17 Monopoli MP, Aberg C, Salvati A, Dawson KA. Biomolecular coronas provide the biological identity of nanosized materials. *Nat. Nanotechnol.* 7(12), 779–786 (2012).

18 Casals E, Pfaller T, Duschl A, Oostingh GJ, Puntes V. Time evolution of the nanoparticle protein corona. *ACS Nano.* 4(7), 3623–3632 (2010).

19 Nagayama S, Ogawara K, Fukuoka Y, Higaki K, Kimura T. Time-dependent changes in opsonin amount associated on nanoparticles alter their hepatic uptake characteristics. *Int. J. Pharm.* 342(1–2), 215–221 (2007).

20 Jansch M, Stumpf P, Graf C, Ruhl E, Muller RH. Adsorption kinetics of plasma proteins on ultrasmall superparamagnetic iron oxide (USPIO) nanoparticles. *Int. J. Pharm.* 428(1–2), 125–133 (2012).

21 Tenzer S, Docter D, Kuharev J *et al.* Rapid formation of plasma protein corona critically affects nanoparticle pathophysiology. *Nat. Nanotechnol.* 8(10), 772–781 (2013).

22 Owens DE 3rd, Peppas NA. Opsonization, biodistribution, and pharmacokinetics of polymeric nanoparticles. *Int. J. Pharm.* 307(1), 93–102 (2006).

23 Lesniak A, Fenaroli F, Monopoli MP, Aberg C, Dawson KA, Salvati A. Effects of the presence or absence of a protein corona on silica nanoparticle uptake and impact on cells. *ACS Nano.* 6(7), 5845–5857 (2012).

• **The serum corona is shown to strongly decrease the association of amorphous silica NPs with cell lines.**

24 Ehrenberg MS, Friedman AE, Finkelstein JN, Oberdorster G, McGrath JL. The influence of protein adsorption on nanoparticle association with cultured endothelial cells. *Biomaterials* 30(4), 603–610 (2009).

•• **Discusses the crucial issue of the specific effects of the various components of the NP corona in serum. The conclusion is that, in endothelial cells, the identity of the NP-bound protein is not relevant.**

25 Barran-Berdon AL, Pozzi D, Caracciolo G *et al.* Time evolution of nanoparticle–protein corona in human plasma: relevance for targeted drug delivery. *Langmuir* 29(21), 6485–6494 (2013).

26 Deng ZJ, Liang M, Monteiro M, Toth I, Minchin RF. Nanoparticle-induced unfolding of fibrinogen promotes Mac-1 receptor activation and inflammation. *Nat. Nanotechnol.* 6(1), 39–44 (2011).

27 Costantini LM, Gilberti RM, Knecht DA. The phagocytosis and toxicity of amorphous silica. *PLoS ONE* 6(2), e14647 (2011).

28 Park EJ, Park K. Oxidative stress and proinflammatory responses induced by silica nanoparticles *in vivo* and *in vitro*. *Toxicol. Lett.* 184(1), 18–25 (2009).

29 Chang JS, Chang KL, Hwang DF, Kong ZL. *In vitro* cytotoxicitiy of silica nanoparticles at high concentrations strongly depends on the metabolic activity type of the cell line. *Environ. Sci. Technol.* 41(6), 2064–2068 (2007).

30 Peters R, Kramer E, Oomen AG *et al.* Presence of nano-sized silica during *in vitro* digestion of foods containing silica as a food additive. *ACS Nano.* 6(3), 2441–2451 (2012).

•• **Shows the likely exposure of men to nanosized amorphous silica after food ingestion.**

31 Tavano R, Franzoso S, Cecchini P *et al.* The membrane expression of *Neisseria meningitidis* adhesin A (NadA) increases the proimmune effects of MenB OMVs on human macrophages, compared with NadA-OMVs, without further stimulating their proinflammatory activity on circulating monocytes. *J. Leukoc. Biol.* 86(1), 143–153 (2009).

32 Zinchuk V, Zinchuk O, Okada T. Quantitative colocalization analysis of multicolor confocal immunofluorescence microscopy images: pushing pixels to explore biological phenomena. *Acta Histochem. Cytochem.* 40(4), 101–111 (2007).

33 Forgac M. Vacuolar ATPases: rotary proton pumps in physiology and pathophysiology. *Nat. Rev. Mol. Cell Biol.* 8(11), 917–929 (2007).

34 Bowman EJ, Siebers A, Altendorf K. Bafilomycins: a class of inhibitors of membrane ATPases from microorganisms, animal cells, and plant cells. *Proc. Natl Acad. Sci. USA* 85(21), 7972–7976 (1988).

35 Rabuffetti M, Sciorati C, Tarozzo G, Clementi E, Manfredi AA, Beltramo M. Inhibition of caspase-1-like activity by Ac–Tyr–Val–Ala–Asp–chloromethyl ketone induces long-lasting neuroprotection in cerebral ischemia through apoptosis reduction and decrease of proinflammatory cytokines. *J. Neurosci.* 20(12), 4398–4404 (2000).

36 Ferrari D, Pizzirani C, Adinolfi E *et al.* The P2X7 receptor: a key player in IL-1 processing and release. *J. Immunol.* 176(7), 3877–3883 (2006).

37 Kahlenberg JM, Dubyak GR. Mechanisms of caspase-1 activation by P2X7 receptor-mediated K^+ release. *Am. J. Physiol. Cell. Physiol.* 286(5), C1100-8 (2004).

38 Netea MG, Simon A, van de Veerdonk F, Kullberg BJ, Van der Meer JW, Joosten LA. IL-1beta processing in host defense: beyond the inflammasomes. *PLoS Pathog.* 6(2), e1000661 (2010).

39 Perregaux DG, McNiff P, Laliberte R, Conklyn M, Gabel CA. ATP acts as an agonist to promote stimulus-induced secretion of IL-1 beta and IL-18 in human blood. *J. Immunol.* 165(8), 4615–4623 (2000).

40 Lynch I, Cedervall T, Lundqvist M, Cabaleiro-Lago C, Linse S, Dawson KA. The nanoparticle–protein complex as a biological entity; a complex fluids and surface science challenge for the 21st century. *Adv. Colloid Interface Sci.* 134–135, 167–174 (2007).

41 Lartigue L, Wilhelm C, Servais J *et al.* Nanomagnetic sensing of blood plasma protein interactions with iron oxide nanoparticles: impact on macrophage uptake. *ACS Nano.* 6(3), 2665–2678 (2012).

•• **Shows how the plasma proteins induce different aggregation states of iron oxide NPs, thus influencing their uptake by macrophages.**

42 Sabuncu AC, Grubbs J, Qian S, Abdel-Fattah TM, Stacey MW, Beskok A. Probing nanoparticle interactions in cell culture media. *Colloids Surf. B Biointerfaces* 95, 96–102 (2012).

43 Maiorano G, Sabella S, Sorce B *et al.* Effects of cell culture media on the dynamic formation of protein–nanoparticle complexes and influence on the cellular response. *ACS Nano*. 4(12), 7481–7491 (2010).

44 Dell'Orco D, Lundqvist M, Oslakovic C, Cedervall T, Linse S. Modeling the time evolution of the nanoparticle–protein corona in a body fluid. *PLoS ONE* 5(6), e10949 (2010).

•• **The interaction and importance of the presence of high-density lipoprotein (HDL), albumin and fibrinogen in the NP corona are investigated.**

45 Cedervall T, Lynch I, Foy M *et al.* Detailed identification of plasma proteins adsorbed on copolymer nanoparticles. *Angew. Chem. Int. Ed. Engl.* 46(30), 5754–5756 (2007).

• **HDL is shown to bind with higher affinity than albumin to copolymer NPs.**

46 Forte TM, Bell-Quint JJ, Cheng F. Lipoproteins of fetal and newborn calves and adult steer: a study of developmental changes. *Lipids* 16(4), 240–245 (1981).

47 Shi J, Hedberg Y, Lundin M, Odnevall Wallinder I, Karlsson HL, Moller L. Hemolytic properties of synthetic nano- and porous silica particles: the effect of surface properties and the protection by the plasma corona. *Acta Biomater.* 8(9), 3478–3490 (2012).

• **The intrinsic ability of silanols to destabilize the cellular plasma membrane is shown, together with their shielding by plasma proteins.**

48 Sahai N. Biomembrane phospholipid–oxide surface interactions: crystal chemical and thermodynamic basis. *J. Colloid Interface Sci*. 252(2), 309–319 (2002).

49 Tenzer S, Docter D, Rosfa S *et al.* Nanoparticle size is a critical physicochemical determinant of the human blood plasma corona: a comprehensive quantitative proteomic analysis. *ACS Nano*. 5(9), 7155–7167 (2011).

•• **The first evidence showing the selective enrichment of human plasma protein on the surface of amorphous silica NPs and its modulation by particle size.**

50 Hellstrand E, Lynch I, Andersson A *et al.* Complete high-density lipoproteins in nanoparticle corona. *FEBS J.* 276(12), 3372–3381 (2009).

• **Biochemical demonstration that complete HDL is indeed recruited on the NP corona.**

51 Lundqvist M, Stigler J, Elia G, Lynch I, Cedervall T, Dawson KA. Nanoparticle size and surface properties determine the protein corona with possible implications for biological impacts. *Proc. Natl. Acad. Sci. USA* 105(38), 14265–14270 (2008).

• **The observation of coronas with different compositions on polystyrene NPs with different surface properties suggests that they may mediate diverse biological effects.**

52 Wang F, Yu L, Monopoli MP *et al.* The biomolecular corona is retained during nanoparticle uptake and protects the cells from the damage induced by cationic nanoparticles until degraded in the lysosomes. *Nanomedicine* 9(8), 1159–1168 (2013).

•• **The cytotoxic action of cationic particles in serum was shown to be mediated by the endosomal-dependent intracellular degradation of the corona, while in the absence of serum it was direct on the plasma membrane.**

53 Seshadri S, Duncan MD, Hart JM, Gavrilin MA, Wewers MD. Pyrin levels in human monocytes and monocyte-derived macrophages regulate IL-1beta processing and release. *J. Immunol.* 179(2), 1274–1281 (2007).

54 Salvati A, Pitek AS, Monopoli MP *et al.* Transferrin-functionalized nanoparticles lose their targeting capabilities when a biomolecule corona adsorbs on the surface. *Nat. Nanotechnol*. 8(2), 137–143 (2013).

• **Highlights how the plasma corona can interfere with specific targeting ligands linked to the NPs' surface.**

55 Lesniak A, Campbell A, Monopoli MP, Lynch I, Salvati A, Dawson KA. Serum heat inactivation affects protein corona composition and nanoparticle uptake. *Biomaterials* 31(36), 9511–9518 (2010).

56 Laurent S, Burtea C, Thirifays C, Rezaee F, Mahmoudi M. Significance of cell 'observer' and protein source in nanobiosciences. *J. Colloid Interface Sci*. 392, 431–445 (2013).

10.2217/NNM.14.22